Available online at www.sciencedirect.com
ScienceDirect
Developmental Biology 299 (2006) 122 – 136
DEVELOPMENTAL BIOLOGY
www.elsevier.com/locate/ydbio

The Grainyhead-like epithelial transactivator Get-1/Grhl3 regulates epidermal terminal differentiation and interacts functionally with LMO4

Zhengquan Yu [a], Kevin K. Lin [a], Ambica Bhandari [a], Joel A. Spencer [a], Xiaoman Xu [a], Ning Wang [a], Zhongxian Lu [a], Gordon N. Gill [b], Dennis R. Roop [c], Philip Wertz [d], Bogi Andersen [a,*]

[a] *Departments of Medicine and Biological Chemistry, University of California, Irvine, Sprague Hall, Room 206, Irvine, CA 92697-4030, USA*
[b] *Department of Medicine, University of California, San Diego, La Jolla, CA 92093, USA*
[c] *Department of Molecular and Cellular Biology, Baylor College of Medicine, Houston, TX 77030, USA*
[d] *Dows Institute, University of Iowa, Iowa City, IA 52242, USA*

Received for publication 13 March 2006; revised 11 July 2006; accepted 12 July 2006
Available online 21 July 2006

Abstract

Defective permeability barrier is an important feature of many skin diseases and causes mortality in premature infants. To investigate the control of barrier formation, we characterized the epidermally expressed Grainyhead-like epithelial transactivator (Get-1)/Grhl3, a conserved mammalian homologue of Grainyhead, which plays important roles in cuticle development in *Drosophila*. Get-1 interacts with the LIM-only protein LMO4, which is co-expressed in the developing mammalian epidermis. The epidermis of *Get-1*$^{-/-}$ mice showed a severe barrier function defect associated with impaired differentiation of the epidermis, including defects of the stratum corneum, extracellular lipid composition and cell adhesion in the granular layer. The *Get-1* mutation affects multiple genes linked to terminal differentiation and barrier function, including most genes of the epidermal differentiation complex. *Get-1* therefore directly or indirectly regulates a broad array of epidermal differentiation genes encoding structural proteins, lipid metabolizing enzymes and cell adhesion molecules. Although deletion of the *LMO4* gene had no overt consequences for epidermal development, the epidermal terminal differentiation defect in mice deleted for both *Get-1* and *LMO4* is much more severe than in *Get-1*$^{-/-}$ mice with striking impairment of stratum corneum formation. These findings indicate that the *Get-1* and *LMO4* genes interact functionally to regulate epidermal terminal differentiation.

Keywords: Get-1; LMO4; Epidermal differentiation; Epidermal differentiation complex; Epidermal barrier; Grainyhead

Introduction

The stratified mammalian epidermis develops from somatic ectoderm late in embryogenesis. As keratinocytes move from the proliferating basal cell layer towards the surface, they undergo a series of differentiation steps to form morphologically distinct suprabasal layers: the spinous, granular and cornified layers. One of the key roles of this process is to form an effective permeability barrier, which depends on several components of the cornified and granular layer (Candi et al., 2005). As a consequence of defective epidermal differentiation, premature infants suffer both from increased transepidermal water loss and percutaneous absorption of chemicals, as well as a fragile skin (Shwayder and Akland, 2005). Barrier function is also defective in several hereditary and acquired inflammatory skin diseases (Nickoloff, 2006).

The cornified envelope is composed of a complex of cross-linked structural proteins that form a rigid structure in the dead cells of the cornified layer. These cells are surrounded by lipid lamellae composed of a mixture of lipids, some of which are cross-linked to the cornified envelope. Cross-linking enzymes such as transglutaminases and metabolic enzymes expressed in the granular layer are responsible for protein cross-linking and

* Corresponding author. Fax: +1 949 824 2200.
E-mail address: bogi@uci.edu (B. Andersen).

0012-1606/$ - see front matter © 2006 Elsevier Inc. All rights reserved.
doi:10.1016/j.ydbio.2006.07.015

lipid synthesis. In addition, cell–cell adhesion molecules in the granular layer, including desmosomes and tight junction proteins, are critical for an effective barrier (Segre, 2003).

Very little is known about the coordinated regulation of gene expression that is required for formation of the epidermal barrier (Segre, 2003). In an effort to understand transcriptional regulation of epidermal differentiation, we previously identified two interacting proteins in the developing epidermis: the LIM-only factor LMO4 and Grainyhead-like epithelial transactivator (Get-1; also referred to as Grainyhead-like transcription factor 3/Grhl3) (Kudryavtseva et al., 2003; Sugihara et al., 1998). LMO4 is a transcriptional co-regulator thought to coordinate larger transcriptional complexes by interacting with DNA-binding proteins (Sugihara et al., 1998). Get-1 is a conserved mammalian homologue of the DNA-binding protein Grainyhead (Kudryavtseva et al., 2003; Ting et al., 2003b), which plays an important role in *Drosophila* cuticle formation (Bray and Kafatos, 1991; Mace et al., 2005). The conserved expression of *Drosophila* Grainyhead and Get-1 suggested a role for Get-1 in mammalian epidermis formation (Kudryavtseva et al., 2003).

During embryonic development of the epidermis, Get-1 and LMO4 are co-expressed in the epidermal keratinocytes and interact *in vitro* (Kudryavtseva et al., 2003), suggesting that both Get-1 and LMO4 might be important for epidermal differentiation. To test this prediction, we studied epidermal development in mice deleted for *Get-1* and *LMO4*. *Get-1* deletion disrupted terminal differentiation and barrier function of the epidermis. Ting et al. (2005) suggested that down-regulation of transglutaminase 1 (Tgm1), a key cross-linking enzyme in epidermal differentiation, is responsible for the epidermal barrier defect and impaired wound healing in *Get-1*$^{-/-}$ mice. In contrast, we found that *Get-1* regulates multiple components of the epidermal barrier in addition to Tgm1, including structural and cell adhesion genes, as well as the lipid component. Furthermore, knockout of *LMO4* enhanced the terminal differentiation defect in *Get-1*$^{-/-}$ mice, indicating functional interactions between *Get-1* and *LMO4* in the regulation of the terminal differentiation program in the epidermis.

Materials and methods

Generation of Get-1$^{-/-}$ *and LMO4*$^{-/-}$ *mice*

A gene-targeting vector was constructed using PCR from 129/SvJae mouse genomic DNA. A 5′ homology arm (3602 bp), a 3′ homology arm (2891 bp) and a loxP arm (2257 bp) were isolated and cloned into the pFOz (3L) vector. The linearized targeting vector was introduced into ES cells by electroporation. Electroporated C57Bl/6J ES cells were grown on selection medium containing G418 (GIBCO BRL). G418-resistant ES cells were isolated and screened by Southern blotting of *Kpn*I-digested genomic DNA with 5′ and 3′ probes, and positive ES cell clones were used to generate the *Get-1* chimeric mice. The chimeric mice were intercrossed with C57Bl/6J mice to obtain *Get-1* floxed mice. The *Get-1* heterozygous knockout mice were obtained by crossing the floxed mice with a Cre-deletor (Schwenk et al., 1995) to remove the DNA fragment from exon 4 to exon 7. The generation of *LMO4*$^{-/-}$ mice was previously described (Lee et al., 2005). Sequences of oligonucleotides used for genotyping and RT-PCR of Get-1 mRNA are provided in Supplementary Table 1.

RT-PCR analysis

Semi-quantitative RT-PCR was performed on total RNA prepared from E18.5 backskin of WT and *Get-1*$^{-/-}$ embryos using Trizol Reagent (Invitrogen) and the High Capacity cDNA Archive Kit (Applied Biosystems). Reactions were sampled after 25, 28 and 30 cycles at different PCR conditions to monitor product accumulation. Sequence of primers is in Supplementary Table 1.

Histology, immunohistology and BrdU staining

Backskin was fixed in 10% formalin, paraffin-embedded and 6-μm sections were stained with hematoxylin and eosin (H&E). For immunohistochemistry, skin tissues were fixed in 6 parts 100% Ethanol, 3 parts water and 1 part Formaldehyde. Antigen-retrieval was performed by heating slides to 95°C for 10 min in 0.01 M citrate buffer (pH 6) in a microwave oven. The sections were then immunostained by the ABC peroxidase method (vector) with diaminobenzidine as the enzyme substrate and hematoxylin as a counterstain. For immunofluorescence, 6-μm-thick fresh frozen sections were air-dried and then washed with PBS. Later, these sections were soaked in blocking solution for 30 min, incubated with occludin mAb for 2 h, washed three times with blocking solution, then incubated with FITC anti-rat IgG pAb (Oncogene Research Products) and counterstained with DAPI in mounting media. For BrdU detection, BrdU (0.05 mg/g) was injected intraperitoneally 2 h prior to sacrifice of the pregnant mother. Embryos were fixed in 10% buffered formalin and paraffin embedded. Slides were pre-treated in 1 M HCl for 1 h at 37°C prior to adding antibody. The primary antibodies used in immunostaining were as follows: rabbit anti-mouse MK5 (Covance), mouse anti-human cytokeratin 10 (DakoCytomation), rabbit anti-mouse filaggrin (Covance), rabbit anti-mouse loricrin (Covance), mouse anti-mouse occludin (Zymed), rabbit anti-mouse claudin 1 (Abcam), rabbit anti-mouse claudin 4 (Abcam), rabbit anti-mouse caspase 14 (Abcam), Rabbit anti-mouse involucrin (Covance) and anti-bromodeoxyuridine (Roche).

In situ hybridization

In situ hybridization studies with ^{35}S-labeled cRNA probes were performed on frozen sections counterstained with bisbenzamide as described previously (Andersen et al., 1995).

Epidermal barrier permeability assay

To assess the epidermal permeability barrier, we used the skin permeability assay described previously (Hardman et al., 1998). After staining, the embryos were photographed using a Nikon E995 digital camera.

Transmission electron microscopy

Fresh skin was dissected into small pieces and fixed by immersion in 2% paraformaldehyde and 2.5% glutaraldehyde in 0.1 M PBS (pH 7.4). Tissues were fixed in room temperature and then washed for four times with PBS. They were postfixed with 0.2% ruthenium tetroxide (RuO_4) and dehydrated through graded ethanol series and embedded in agar 100 resin. Ultrathin sections were contrasted with uranyl acetate and lead citrate and examined on a transmission electron microscope.

Preparation of cornified envelopes (CEs) and sonication experiments

Embryo skin was processed with dispase at 37°C for 30 min and epidermis was isolated. CEs were prepared by heating epidermis at 95°C for 10 min in preheated extraction buffer (0.1 M Tris pH 8.5, 2% SDS, 20 mM DTT, 5 mM EDTA pH 7.5). CEs were collected by centrifugation of 5000×*g* for 15 min and stored in 500 μl extraction buffer. For sonication, CEs were diluted in extraction buffer and the CE suspension was sonicated in Eppendorf tubes on ice for different time points. CE aliquots were photographed.

Lipid analysis

Epidermis was isolated from e18.5 WT, heterozygous and Get-1 knockout embryos as described above. Lipid analysis from pooled epidermis preparations was performed as previously described (Law et al., 1995). Similar results were obtained in four independent experiments.

RNA isolation and microarray experiments

The same region of the mouse backskin was excised from three *Get1-1*$^{+/+}$ and three *Get1-1*$^{-/-}$ mice at e18.5. Microarray experiments were performed as previously described except we used Affymetrix Murine Genome 430 2.0 arrays (45,037 probe sets) and washed according to manufacturer's recommendations (Affymetrix, Santa Clara, CA) (Lin et al., 2004).

Cyber-T analysis

After excluding absent genes, the raw expression values from replicate samples were analyzed by the Cyber-T program (Baldi and Long, 2001), which identifies statistically significant differentially expressed genes. We implemented the following filtering criterion to exclude absent genes from subsequent analysis: all three replicate samples of either Get1-1$^{+/+}$ or Get1-1$^{-/-}$ mice must have "present" or "marginally present" calls, as determined by MAS 5.0. To determine the global false positive rate inherent in multiple hypotheses testing

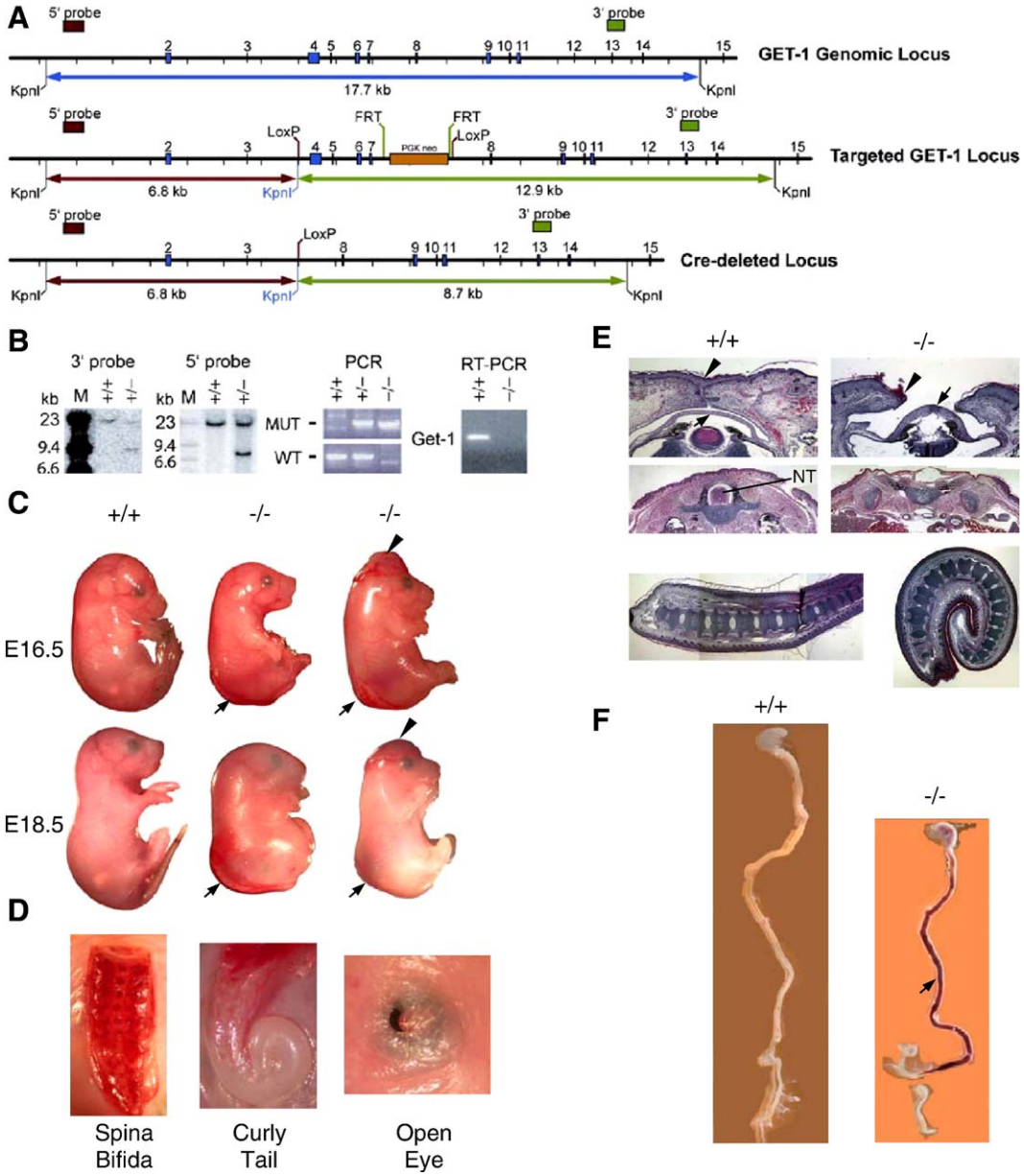

Fig. 1. Generation and phenotypes of *Get-1*$^{-/-}$ mice. (A) Strategy for targeted deletion of the *Get-1* gene. Exons are represented as boxes. Locations of probes for Southern blots are indicated. (B) The first two panels show Southern blot analysis of *Kpn*I-digested genomic DNA from WT (+/+) and targeted (+/−) embryonic cells with 3′ and 5′ probes. The third panel shows PCR identification of genotypes of mice using primers detecting normal (WT) and deleted (MUT) *Get-1* loci. The fourth panel shows absence of Get-1 mRNA in *Get-1*$^{-/-}$ mice by RT-PCR. (C) Appearance of *Get-1*$^{-/-}$ mice at e16.5 and e18.5. Arrowheads indicate exencephaly and arrows indicate spina bifida. (D) Higher magnification images of spina bifida, curly tail and open-eye phenotypes in *Get-1*$^{-/-}$ mice. (E) Histology of e18.5 embryos shows open-eye, spina bifida and curly tail phenotypes. Arrowheads point to the eyelid closure front and arrows point to the cornea. (F) Overview of the intestine of *Get-1*$^{-/-}$ mice. Arrow points to blood in intestine.

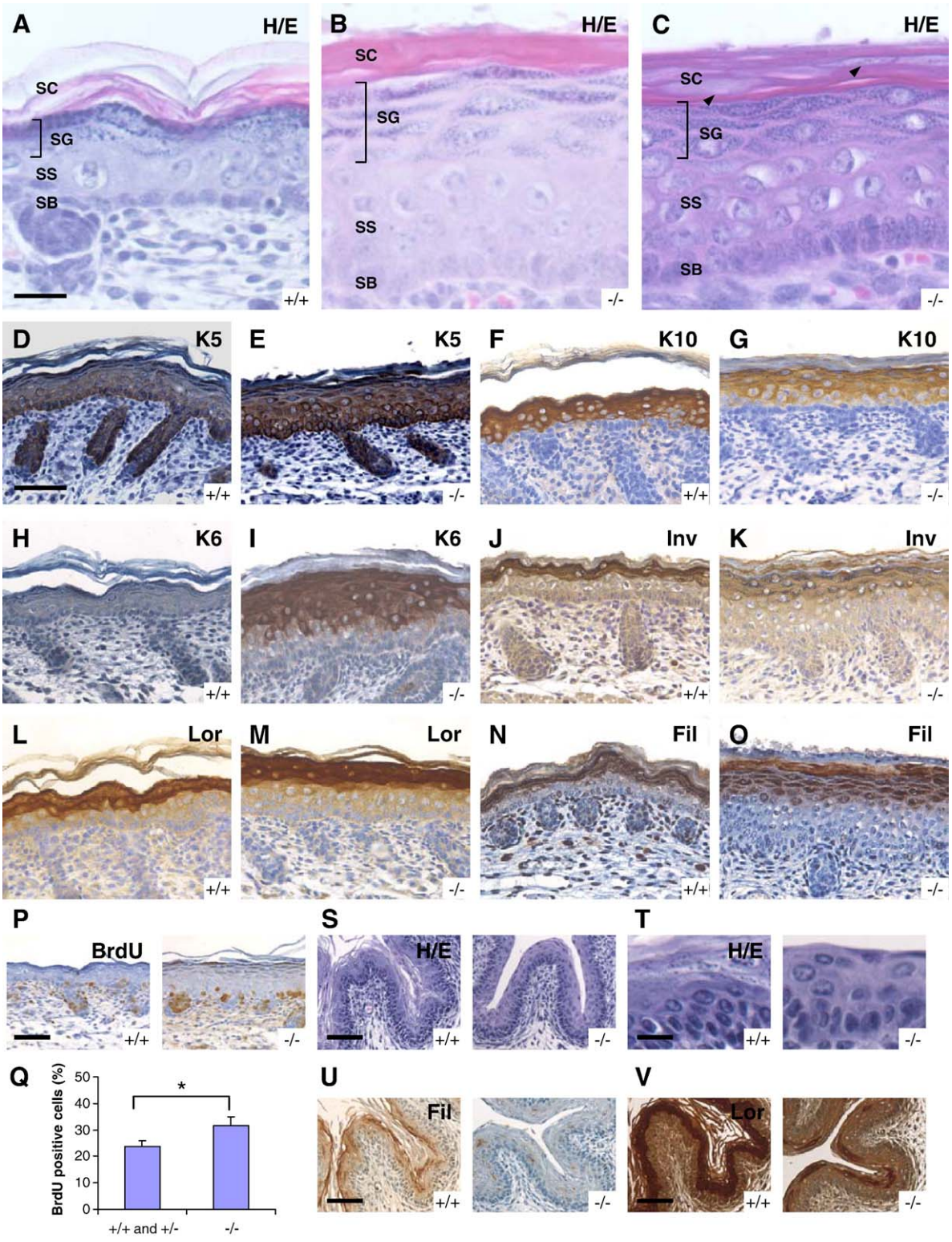

Fig. 2. Impaired epithelial differentiation in *Get-1*$^{-/-}$ epidermis and forestomach. (A–C) Histological analysis of e18.5 backskin from WT (A) and *Get-1*$^{-/-}$ (B–C) embryos. Arrowheads in C point to nuclei in the stratum corneum. (D–O) Immunostaining analysis of e18.5 backskin from WT (D, F, H, J, L and N) and *Get-1*$^{-/-}$ (E, G, I, K, M and O) embryos. Antibodies to the following keratinocyte differentiation markers were used, K5 (D–E), K10 (F–G), K6 (H–I), involucrin (J–K), loricrin (L–M) and filaggrin (N–O). (P) BrdU staining of e18.5 backskin from WT (left panel) and *Get-1*$^{-/-}$ (right panel) embryos. (Q) The ratio of BrdU positive cells in the basal cell layer of e18.5 backskin with the indicated genotypes. Results represent mean and standard error. The asterisk denotes statistically significant difference between WT/heterozygous and *Get 1*$^{-/-}$ mice ($P < 0.02$). (S) Histological analysis of forestomach epithelium from e18.5 mice with the indicated genotypes. (T) Higher magnification of the images shown in S. (U) Filaggrin immunostaining of forestomach epithelium from e18.5 mice with the indicated genotypes. (V) Loricrin immunostaining of forestomach epithelium from e18.5 mice with the indicated genotypes. Scale bars: A–C, 25 μm; D–S, U and V, 50 μm; T, 12.5 μm. H/E, hematoxylin/eosin staining; SB, basal layer; SC, cornified layer; SG, granular layer; SS, spinous layer.

of high-dimensional DNA array data, the posterior probability of differential expression (PPDE) was calculated using the *P* values of log-transformed data. The PPDE for the selected cut-off *P* value of 0.0025 is 0.80, which indicates that the false discovery rate is within 20%. Overrepresented gene ontology biological process categories and chromosomal band localization for differentially expressed genes were determined using the DAVID (Database for Annotation, Visualization and Integrated Discovery) 2.0 program (Dennis et al., 2003).

Batch extraction and analysis of cis-regulatory regions (BEARR)

BEARR was used to determine the possible Get-1 binding sequence using position weight matrix score (PWM score ≥6.73) by extracting the promoter regions (2 kb upstream region of transcription start site) of significantly altered genes in the microarray (Vega et al., 2004). The PWM input used for the analysis was from the core Get-1 DNA binding consensus sequence (AACCGGTT) derived from a previously published CASTing results (Ting et al., 2005). The sequence and annotation database selected for BEARR analysis was the Mouse Genome Assembly NCBI Build 33. Of the 162 unique genes identified by Cyber-T to be downregulated, BEARR was able to obtain 2 kb upstream sequence for 136 genes, and 35 of these genes (25.7%) have sites with PWM scores ≥6.73. Of the 69 unique genes identified by Cyber-T to be upregulated, BEARR was able to obtain 2 kb upstream sequence for 59 genes, and 12 of these genes (20.3%) have sites with PWM scores ≥6.73. To estimate the expected number of genes identified to have upstream sites with PWM scores ≥6.73 by chance (false positives), we systematically performed PWM analysis on statistically significant non-regulated genes by Get-1 ($P>0.99$ from Cyber-T analysis; 246 probe sets, corresponding to 192 unique genes). For these non-regulated genes, BEARR was able to obtain 2 kb upstream sequence for 173 genes, and 31 of these genes (17.9%) have sites with PWM scores ≥6.73. In running the ConSite program (Sandelin et al., 2004), we used 75% as the cut-off threshold for conservation of Get-1 binding sites and genomic regions with a sliding window of 50 bp.

Electrophoretic mobility shift assay (EMSA)

Sequences extracted by BEARR were used as unlabeled competitor oligonucleotides in the competition EMSA (Supplementary Table 2). Get-1 protein (0.2 ng/ml) was incubated with [γ^{32}]P-labeled duplex Get-1 consensus sequence (TCCTGTTAAACCGGTTTTTCTAGT) and EMSA performed as previously described (Kudryavtseva et al., 2003). The DNA-protein complexes in the various bands were quantified by cutting them out and measuring their counts using a scintillation counter. Data were expressed as percent binding relative to that determined in the absence of a competitor. A competitive binding curve was used to approximate the concentration of the unlabelled oligonucleotides (IC_{50}) required for 50% inhibition of binding. The computed relative affinity is the IC_{50} of the gene relative to the IC_{50} of Tgm1.

Co-immunoprecipitations and Western blots

Expression plasmids, pCS2-MT-LMO4 and pCDNA-HA-Get-1 were transiently transfected into HEK293T cells and cell extracts prepared as previously described (Lu et al., 2006). Cell extracts were precipitated with an HA antibody (Covance; MMS-101R) and Western blots were performed with MT antibody (Upstate; 06-340). Input extracts were analyzed by Western blots with the same antibodies.

Results

Get-1 regulates terminal differentiation of the epidermis and the forestomach epithelium

To test whether Get-1 and LMO4 play roles in epidermal development, we studied mice deleted for *Get-1* and *LMO4*. We first generated *Get-1*$^{-/-}$ mice lacking exons 4 to 7, which encode for the activation domain and part of the DNA-binding

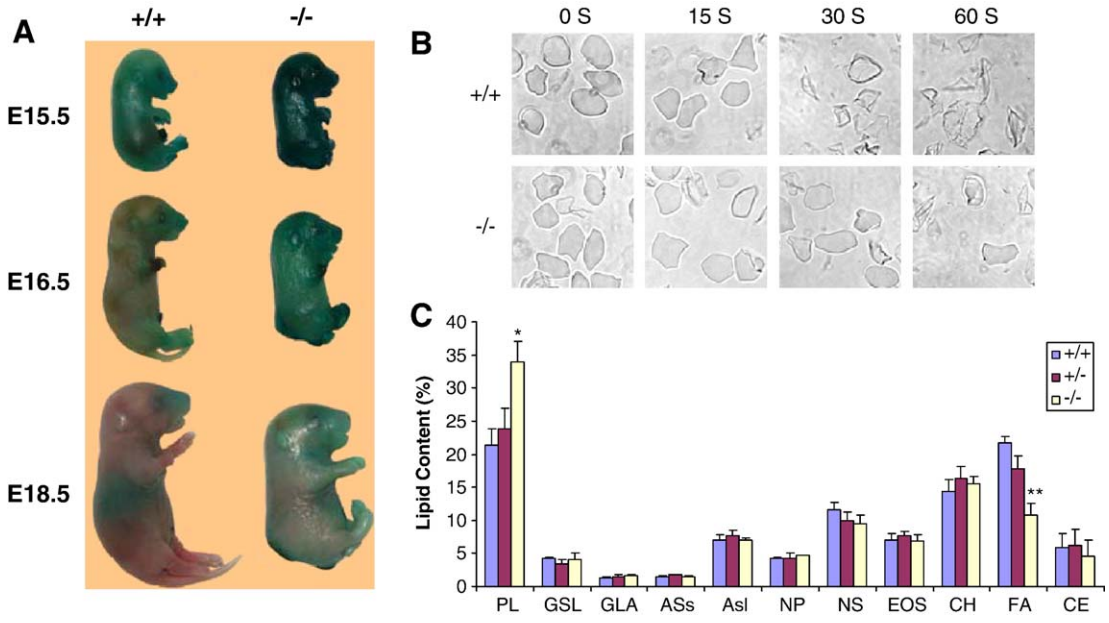

Fig. 3. Defective epidermal permeability barrier and abnormal epidermal lipid composition in *Get-1*$^{-/-}$ mice. (A) Epidermal permeability barrier assay by X-gal staining of mouse embryos of the indicated ages and genotypes. (B) Ultrasound fragility analysis of cornified envelopes isolated from the epidermis of e18.5 mice of the indicated genotypes. Shown are images of cornified envelopes after ultrasound treatment for 0, 15, 30 and 60 s. (C) Lipid composition of epidermis of mice with the indicated genotypes. Shown are means and standard errors from pooled epidermal samples in four different experiments. * and ** denote $P<0.01$ and $P<0.002$, comparing WT and *Get 1*$^{-/-}$ epidermis. PL, phospholipids; GSL, glucosylceramides; GLA, acylglucosylceramide; ASs, ceramide containing sphingosine and short α-hydroxyacids; Asl, ceramide containing sphingosine and long α-hydroxyacids; NP, ceramide containing sphingosine and short α-hydroxyacids; NS, ceramide containing sphingosine and normal fatty acids; EOS, acylceramide consisting of omega-hydroxyacids amide-linked to sphingosine and bearing linoleate ester-linked to the omega-hydroxyl group; CH, cholesterol; FA, fatty acid; SE, cholesterol ester.

domain (Figs. 1A–B). The *Get-1*$^{-/-}$ mice died at birth with neural tube closure defects characterized by spina bifida (100%) and exencephaly (14%), and exhibited tail abnormalities (100%), primarily curly tail (Figs. 1C–E and Supplementary Table 3). These phenotypes are similar to those previously described in mice deleted for part of exon 2 and exon 3 of the *Get-1* gene (Ting et al., 2003a). However, in the present study, the incidence of exencephaly was 7 times higher and additional abnormalities were observed, including an open-eye phenotype (7%; Supplementary Table 3) and shorter intestine with blood in the lumen (Fig. 1F). The mean intestine lengths of WT and *Get 1*$^{-/-}$ mice were 6.8 and 5.9 cm, respectively ($P<0.002$). The eye and gut phenotypes expand the known functions of Get-1.

To understand the role of *Get-1* in epidermal development, we examined skin histology and marker expression in *Get-1*$^{-/-}$ mice from embryonic days (e) 14.5 to 18.5 (Figs. 2A–O and Supplementary Fig. 1). At e14.5, the skin histology was normal but by e16.5 there was thickening of the epidermis, which became more pronounced at e18.5 (Figs. 2A–C and Supplementary Fig. 1). At this stage, the cornified layer was more compact and often contained nuclei (Fig. 2C). The granular layer was thicker due to an increased number of cell layers and the cells of the most superficial layers being more cuboidal than normal. The spinous layer was also thicker and the basal layer appeared disorganized. Keratin 5 and 10 expression appeared normal whereas keratin 6 expression, often associated with increased epidermal proliferation, was strongly upregulated in *Get-1*$^{-/-}$ epidermis, especially close to the spina bifida (Figs. 2D–I). Examination of the terminal differentiation markers involucrin, loricrin and filaggrin revealed that the onset of loricrin expression was delayed at

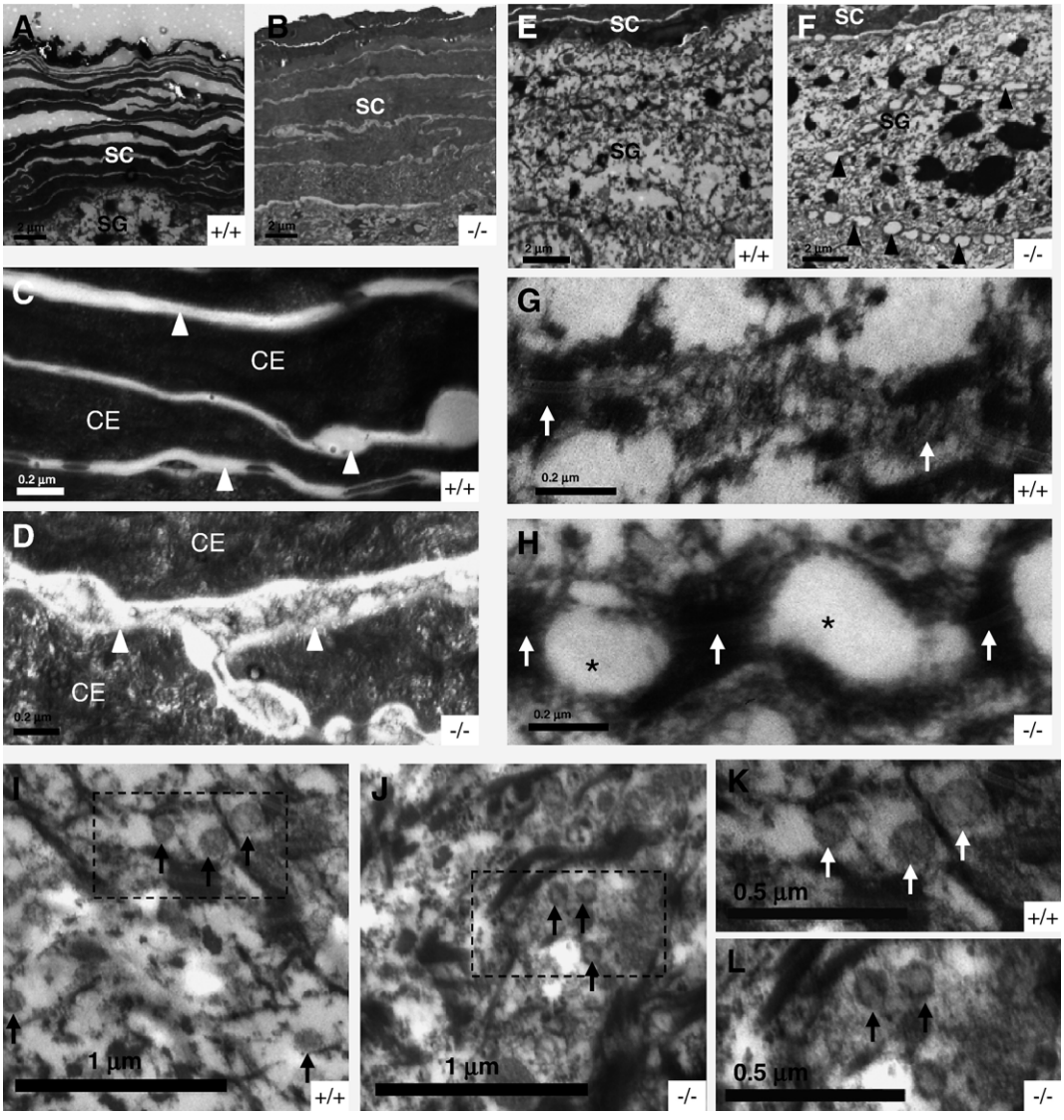

Fig. 4. Ultrastructure of *Get-1*$^{-/-}$ epidermis. (A–B) Stratum corneum of WT (A) and *Get-1*$^{-/-}$ (B) mice at e18.5. (C–D) Higher magnification of WT (C) and *Get-1*$^{-/-}$ (D) stratum corneum. Arrowheads indicate intercellular spaces. (E–F) Granular layer of WT (E) and *Get-1*$^{-/-}$ (F) epidermis from e18.5 embryos. Arrowheads indicate separated cell–cell adhesions in *Get-1*$^{-/-}$ the epidermis. (G–H) Higher magnification of the granular layer of WT (G) and *Get-1*$^{-/-}$ (H) mice. Arrows indicate desmosomes. Asterisks indicate the abnormally separated intercellular spaces. (I–L) Lamellar bodies indicated with arrows in the granular layer of e18.5 epidermis from WT (I–K) and *Get-1*$^{-/-}$ (J–L) embryos. CE, cornified envelope; SC, stratum corneum; SG, granular layer.

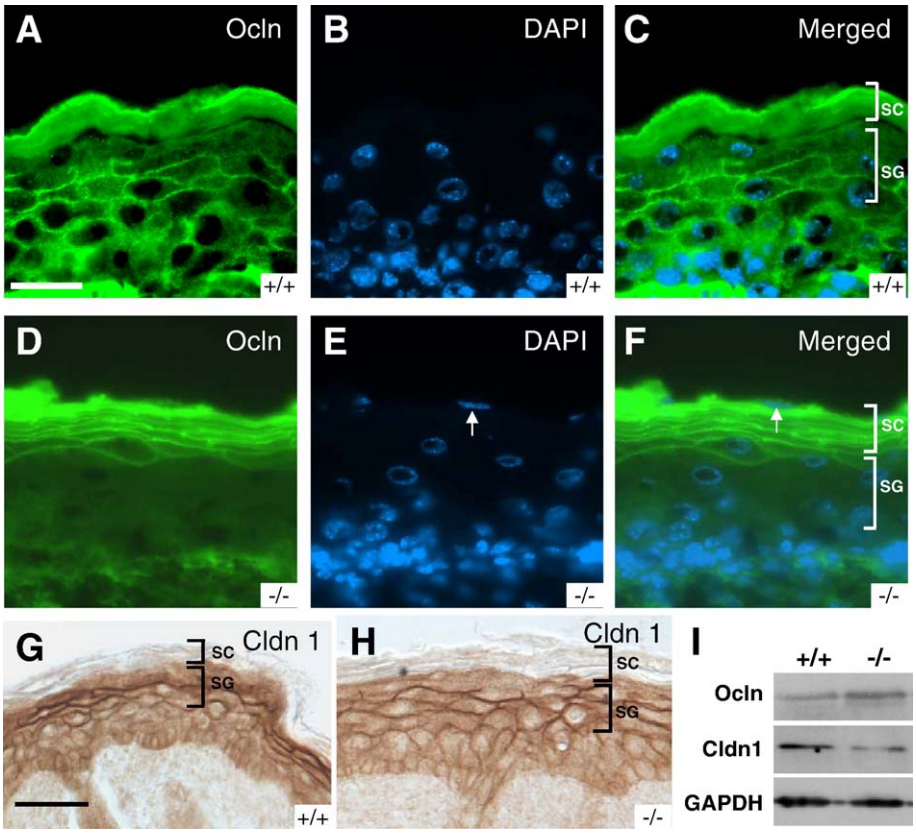

Fig. 5. Expression pattern of occludin and claudin 1 in WT and *Get 1*$^{-/-}$ epidermis. (A) Immunofluorescence analysis of occludin expression in WT epidermis. (B) DAPI staining showing nuclei in the same section as panel A. (C) The merged image of panels A and B. (D) Immunofluorescence analysis of occludin expression in *Get 1*$^{-/-}$ epidermis. (E) DAPI staining showing nuclei in the same section as panel D. (F) The merged picture of panels D and E. (G–H) Immunohistochemistry analysis of claudin 1 expression in WT (G) and *Get 1*$^{-/-}$ (H) epidermis. SC, cornified layer; SG, granular layer. A nucleus in cornified layer is indicated by arrow. (I) Western blot analysis of occludin and claudin 1 in WT and *Get 1*$^{-/-}$ epidermis. Ocln, occludin; Cldn1, claudin 1. Scale bars: panels A–F, 25 μm; G–H, 50 μm.

e14.5 whereas the other two terminal differentiation markers were expressed at the appropriate time (Supplementary Fig. 1). However, all three markers showed an expanded domain of expression at e18.5, corresponding to expansion of the granular layer (Figs. 2J–O). Involucrin expression was decreased slightly at e16.5 (Supplementary Fig. 1) and clearly at e18.5 (Figs. 2J–K). Together, these abnormalities demonstrate altered terminal differentiation of the *Get-1*$^{-/-}$ epidermis. Consistent with epidermal hyperplasia, there was a mild, yet statistically significant increase in keratinocyte proliferation in the basal cell layer of the *Get-1*$^{-/-}$ epidermis (Figs. 2P–Q). The forestomach epithelium, which is similar to the epidermis, showed reduced number of granules in the superficial layers (Figs. 2S–T) and decreased expression of filaggrin and loricrin (Figs. 2U–V), signifying impaired terminal differentiation of the forestomach epithelium. These experiments demonstrate that *Get-1* plays important roles in the differentiation of stratified epithelia of both ectodermal and endodermal origin, thus expanding the role for this mammalian homologue of *Drosophila* Grainyhead.

Get-1 regulates the lipid composition, cell–cell adhesion and barrier function of the epidermis

One key role of the epidermis is the formation of an effective permeability barrier. By performing an *in situ* permeability assay (Hardman et al., 1998), impaired barrier formation was evident in *Get-1*$^{-/-}$ mice at e16.5 and e18.5 (Fig. 3A). An effective barrier depends in part on the structural integrity of the cornified envelope. To test the fragility of cornified envelopes, we exposed them to ultrasound for different time periods. Interestingly, the cornified envelope appeared normal or slightly less

Fig. 6. Deletion of the *Get-1* gene affects the expression of multiple genes crucial for terminal differentiation and barrier function of epidermis. (A) Overview of microarray data processing and Cyber-T analysis to identify statistically significant differentially expressed genes in the backskin of *Get-1*$^{-/-}$ mice. (B) List of differentially expressed genes grouped into functional categories important in epithelial barrier formation. *P* value corresponds to the significance of differential expression as determined by Cyber-T analysis; bold *P* values are highly significant ($P<0.0025$). Asterisk, the probe set corresponding to *Get-1* is outside the deleted exons of *Get-1*$^{-/-}$ mice. (C) Semiquantitative RT-PCR of a random selection of genes from panel B. Asterisk, the primer set used to interrogate the expression of Get-1, is outside the deleted exons of *Get-1*$^{-/-}$ mice. Gapdh and 18S are endogenous controls. (D) Fold changes of gene expression within the epidermal differentiation complex (EDC). For graphical clarity, only genes that are differentially expressed with $P<0.05$ are shown with gene symbol, strand direction and fold change. Dotted lines, boundaries of the EDC.

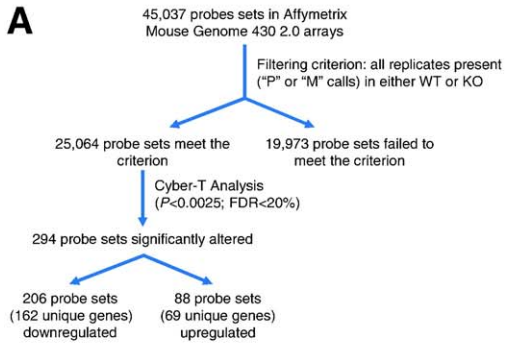

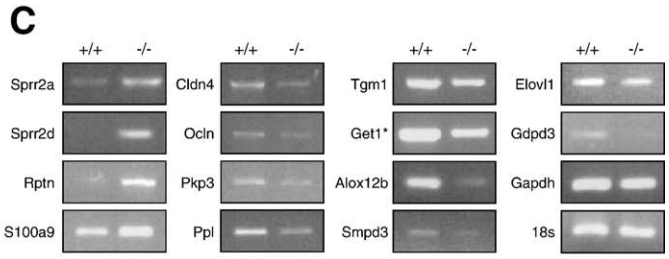

B

UniGene ID	Gene title	Gene symbol	*P* value	Fold
Structural proteins				
Mm.162684	filaggrin	Flg	0.01959	-1.34
Mm.156955	involucrin	Ivl	**0.00211**	-2.14
Mm.1121	loricrin	Lor	**0.00072**	-1.44
Mm.331191	small proline-rich protein 1A	Sprr1a	**0.00233**	-2.71
Mm.6853	small proline-rich protein 2A	Sprr2a	**<0.00001**	4.95
Mm.87820	small proline-rich protein 2D	Sprr2d	**<0.00001**	7.01
Mm.10692	small proline-rich protein 2F	Sprr2f	0.03228	3.45
Mm.10693	small proline-rich protein 2H	Sprr2h	0.02092	1.54
Mm.301748	small proline rich-like 1	Sprrl1	**<0.00001**	5.08
Mm.279773	small proline rich-like 2	Sprrl2	0.02453	-1.34
Mm.41969	small proline rich-like 3	Sprrl3	0.00436	-1.54
Mm.291769	small proline rich-like 5	Sprrl5	0.00513	-1.52
Mm.176243	small proline rich-like 7	Sprrl7	0.00499	-1.55
Mm.23784	small proline rich-like 9	Sprrl9	0.00444	-1.88
Mm.292457	small proline rich-like 10	Sprrl10	**<0.00001**	-3.56
Mm.1417	repetin	Rptn	**<0.00001**	27.71
Mm.703	S100 calcium binding protein A3	S100a3	0.04121	-3.09
Mm.21567	S100 calcium binding protein A8 (calgranulin A)	S100a8	**0.00009**	3.97
Mm.2128	S100 calcium binding protein A9 (calgranulin B)	S100a9	**<0.00001**	4.92
Mm.24006	S100 calcium binding protein A14	S100a14	0.00492	-1.53
Mm.35806	RIKEN cDNA 2300002G24 gene (homolog to human Nice1)	2300002G24Rik	**0.00187**	-1.59
Adhesion molecules				
Mm.289441	claudin 1	Cldn1	**0.00087**	-2.31
Mm.7339	claudin 4	Cldn4	**0.00058**	-2.20
Mm.37817	claudin 23	Cldn23	**0.00024**	-3.01
Mm.4807	occludin	Ocln	**0.00228**	-2.22
Mm.350037	plakophilin 3	Pkp3	**0.00242**	-1.67
Mm.266875	periplakin	Ppl	**0.00009**	-1.80
Mm.293683	envoplakin	Evpl	0.04208	-1.30
Mm.909	desmocollin 1	Dsc1	0.03673	-1.54
Mm.247477	corneodesmosin	Cdsn	0.01393	-1.49
Protein / lipid-modifying enzymes				
Mm.41964	transglutaminase 1, K polypeptide	Tgm1	**0.00195**	-1.81
Mm.20851	peptidyl arginine deiminase, type III	Padi3	0.00489	-2.28
Protease and serine-protease inhibitor				
Mm.20024	similar to human kallikrein 5 preproprotein	1110030O19Rik	**0.00125**	-1.96
Mm.83909	serine (or cysteine) proteinase inhibitor, clade B, member 8	Serpinb8	0.01608	-1.74
Transcription factors				
-	grainyhead like epithelial transactivator 1 *	Get1 / Grhl3	**0.00112**	-2.00
Mm.325445	Skin-1a	Pou2f3 / Skn-1a	**0.00198**	-1.71
Enzymes and transporters involved in lipid metabolism				
Mm.41989	arachidonate lipoxygenase 3	Aloxe3	0.02175	-1.50
Mm.340329	arachidonate 12-lipoxygenase, 12R type	Alox12b	0.00310	-2.17
Mm.5031	glucosidase, beta, acid	Gba	0.04756	-1.30
Mm.4628	sphingomyelin phosphodiesterase 1, acid lysosomal	Smpd1	**0.00001**	-2.03
Mm.23298	sphingomyelin phosphodiesterase 3, neutral	Smpd3	**0.00049**	-3.14
Mm.287187	sphingomyelin phosphodiesterase, acid-like 3B	Smpdl3b	**0.00196**	-2.54
Mm.249342	7-dehydrocholesterol reductase	Dhcr7	0.00446	-1.66
Mm.5092	phospholipase A2, group IB, pancreas, receptor	Pla2g1br	0.03762	1.50
Mm.331989	phospholipase A2, group IIF	Pla2g2f	0.00301	-2.21
Mm.100476	phospholipase A2, group III	Pla2g3	0.00257	-2.14
Mm.87136	Phospholipase A2, group IVB (cytosolic)	Pla2g4b	**0.00097**	-2.22
Mm.180189	diacylglycerol O-acyltransferase 2	Dgat2	**0.00021**	-1.78
Mm.282096	elongation of very long chain fatty acids-like 1	Elovl1	**0.00012**	-1.65
Mm.281887	glycerophosphodiester phosphodiesterase domain containing 1	Gdpd1	**0.00102**	-2.13
Mm.246881	glycerophosphodiester phosphodiesterase domain containing 3	Gdpd3	**<0.00001**	-2.88

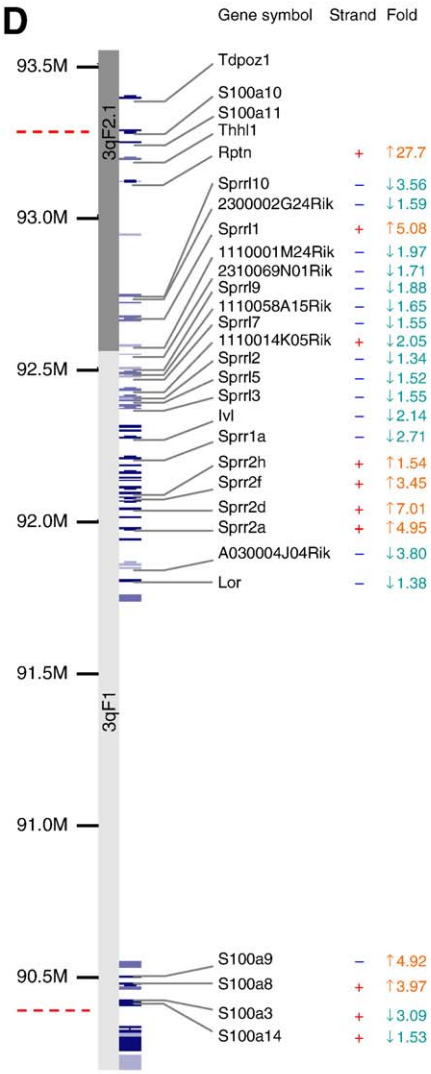

fragile in *Get-1*$^{-/-}$ mice (Fig. 3B), suggesting that the barrier dysfunction is not caused by increased fragility of the cornified envelope. However, we found that the lipid composition of the epidermis was altered with statistically significantly increased phospholipids (PL) and decreased fatty acids (FA), which are implicated in maintaining normal barrier function (Elias, 2005) (Fig. 3C). Because FA are derived from PL, these findings indicate an impairment in the conversion of PL to FA (Fluhr et al., 2001).

To investigate in more detail the epidermal structure of *Get-1*$^{-/-}$ mice, we performed transmission electron microscopy (TEM). These experiments showed that the stratum corneum of the *Get-1*$^{-/-}$ mice was more compact and that the corneocytes were enlarged with irregular surface structure (Figs. 4A–B). The space between the corneocytes, where lipid lamellar layer normally exists, contained residual material not found in wild type (WT) mice (Figs. 4C–D), consistent with abnormalities in lipid composition. Interestingly, intercellular junctions in the top of the granular layer showed abnormal separation of cells between desmosomal regions, creating the appearance of periodic intercellular spaces (Figs. 4E–H). This adhesion abnormality was observed in three out of five knockout mice and not in four WT mice. The lipids synthesized in the cells of the granular layer are packaged into lamellar bodies that are subsequently secreted for use in the intercellular spaces of the stratum corneum. Consistent with abnormal lipid composition, we found that lamellar bodies are decreased in size and optical density in *Get-1*$^{-/-}$ mice (Figs. 4I–L).

Because tight junctions have been shown to be critical for effective epidermal barrier function, we analyzed the epidermal expression of claudin 1, claudin 4 and occludin. As expected, occludin is most highly expressed at the cell surface of keratinocytes in the granular layer of WT mice (Figs. 5A–C). Intriguingly, occludin expression appears displaced from the granular layer but is found aberrantly in the cornified layer of *Get-1*$^{-/-}$ mice (Figs. 5D–F). In contrast, although the pattern of claudin 1 expression appears normal, overall expression appears slightly decreased in the *Get 1*$^{-/-}$ epidermis (Figs. 5G–H). Western blot analysis showed that whereas the skin expression of occludin is increased, claudin 1 protein expression is decreased in the *Get 1*$^{-/-}$ mice (Fig. 5I). In summary, there are abnormalities in the pattern of expression for occludin and altered expression levels for claudin 1. Together, these findings are indicative of multiple causes for the barrier defect of *Get-1*$^{-/-}$ mice, including changes in extracellular lipids and defective cell–cell adhesions in the granular layer.

A

	Probe sets	Unique genes	Promoters retrieved	Binding sites within conserved regions
Downregulated	206	162	137	7
Upregulated	88	69	59	3
Non-regulated	246	192	174	0

B

	Sequence	From	To
Downregulated			
mm6_Anxa9	TGATGGTATGTGTCCC**AACAGGTT**CTTCTCTATCAACCTT	772	779
hg17_Anxa9	TGCTGGTATGTGCCCC**AACAGGTT**TTTCCCTATCAGCCTT	195	202
mm6_Bnipl	GGAGGGGAGGTGGCAA**AACCTGTT**T GAAGATGAGGTTAC	51	58
hg17_Bnipl	GGAGAGGAG TGGCAA**AACCTGTT**TTGAAGATGAGGTTAC	47	54
mm6_2300002G24Rik	CTCTGGTTCAGTAAGC**AACCTGTT**AATCAGGCTCTAAAGC	1135	1142
hg17_c1ORF42 (Nice1)	CTCTAG GAACTGGC**AACCTGTT**AATCAGGCTCTAAATC	1198	1205
mm6_Gsdm1	GAGGCGGGGCACTTCA**AACAGGTT**GATGCTGTTCTCCTGG	123	130
hg17_Gsdm1	GCCAGGGCACACGTGG**AACAGGTT**GATGTTGTTCTCCAGG	81	88
mm6_Gpld1	AAACAACAAAAAGAGA**AGCCGGTT**CTCGGTGATCACCATA	105	112
hg17_Gpld1	AAATACTGAAAAG GA**AGCCAGTT**CCAGCTGATTACCATA	418	425
mm6_Sult2b1	GGGCAGCAGCTGGGAG**AACCGGCT**G TGCCCCTCCC	33	40
hg17_Sult2b1	GGGTAGCAGCTGGGAG**AACCGGCT**GGGTGCTGCCCCTCCC	62	69
mm6_Tgm1	GAGAGTGTGTTCCTGG**AGCCGGTT**GGTCTGGATTCTCAAG	1249	1256
hg17_Tgm1	CAGCACAGGTGCCT G**AGCCGGTT**GGTCTGGATTCCCAGG	854	861
Upregulated			
mm6_Nrk	GAGCGGCGCAGAGCGG**GACCGGTT**TTCCGGGGCTGGCAGC	374	381
hg17_Nrk	GAGCGGCGCGGAGCGA**GACCGGTT**TTCCGGGGCTGGCAGC	320	327
mm6_Rptn	GCATACTACAATGACA**AAACAGGTT**CATGAGCAAACAAGGG	189	196
hg17_Rptn	ACCTACTGTAGTGACA**AAACAGGTT**CATGAGCAAGTGGGGG	178	185
mm6_s100a9	GGGAAGTGAGCCAACT**AACCAGTT**TCCCCCCAAACAAGCT	195	202
hg17_s100a9	GGGAAATGAACTAAAC**AACCAGCT**TCCTCCCAAACCAGTT	225	232

C

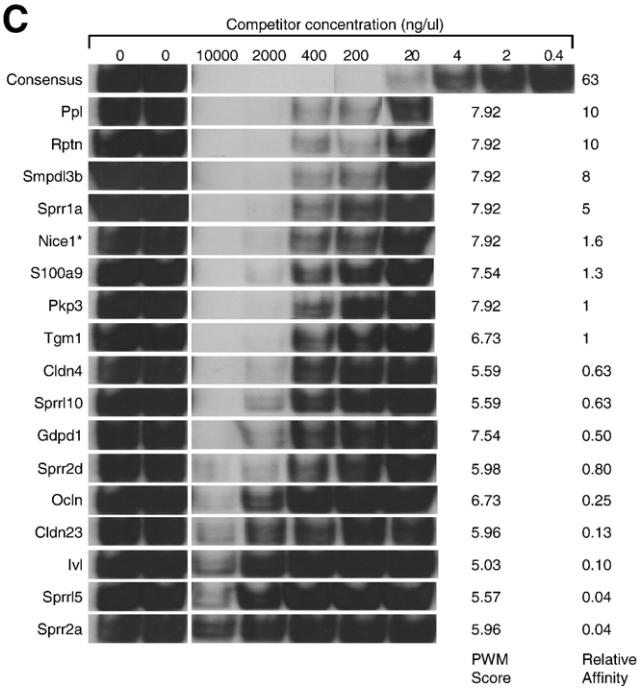

Fig. 7. Identification of evolutionarily conserved Get-1 binding site in promoter regions of *Get-1*-regulated genes. (A) Overview of Get-1 binding site analysis in promoters from differentially expressed genes in *Get-1*$^{-/-}$ epidermis. As a control, we also determined the frequency of Get-1 binding sites in non-regulated genes. (B) Get-1 binding sites in regulated genes. Location of the binding site in relation to the start site is indicated for both human and mouse genes. (C) Electrophoretic mobility shift assays with a ^{32}P-labeled consensus DNA-binding site for the Get-1 protein. Binding was competed with the indicated amounts of unlabeled binding sites from the indicated Get-1-responsive genes. Shown on the right are the probability weight matrix (PWM) scores of potential Get-1 binding sequences as previously determined, and the affinity of each sequence relative to the site found in the Tgm1 gene.

Deletion of the Get-1 gene affects multiple epidermal genes involved in lipid metabolism, cell–cell adhesion and structural integrity of the cornified envelope

To gain insights into the molecular mechanisms of permeability barrier defects in *Get1*$^{-/-}$ mice, we performed expression profiling of backskin RNA from *Get1*$^{-/-}$ and WT mice at e18.5 (Fig. 6A). Using the Cyber-T program (Long et al., 2001) with $P<0.0025$ (false discovery rate <20%), we found that only 294 of the 25,064 expressed probe sets were significantly altered, indicating that deletion of *Get-1* leads to highly selective changes in gene expression. Of the altered probe sets, 206 (162 unique genes) were downregulated, and 88 (69 unique genes) were upregulated (Fig. 6A). A complete list of these genes with corresponding *P*-values is provided in Supplementary Table 4. Strikingly, the great majority of differentially expressed genes play key roles in the terminal differentiation program and barrier formation, including structural proteins of the cornified envelope, cell adhesion molecules and enzymes involved in lipid metabolism (Fig. 6B). A selection of altered genes from different functional groups was validated with semi-quantitative RT-PCR (Fig. 6C).

Systematic statistical analysis of chromosomal location revealed that the significantly downregulated genes were overrepresented in two adjacent chromosomal bands, 3F1 ($P=0.00038$) and 3F2.1 ($P=0.031$). These genes on chromosome 3 fall within the epidermal differentiation complex (EDC), which comprises a large number of genes that encode structural proteins of the cornified envelope (Fig. 6D). Although Get-1 regulates the majority of the genes within the EDC, it is of note that some genes are downregulated whereas others are upregulated. This is in contrast to the Klf4 transcription factor, which represses all *Sprr2* and *Sprr1* genes (Segre et al., 1999), indicating that these two regulatory factors act differently on the EDC. In addition, there is a decrease in the expression of a large number of adhesion molecules, including claudins, occludin, Plakophilin 3 and Periplakin (Fig. 6B) which likely contributes

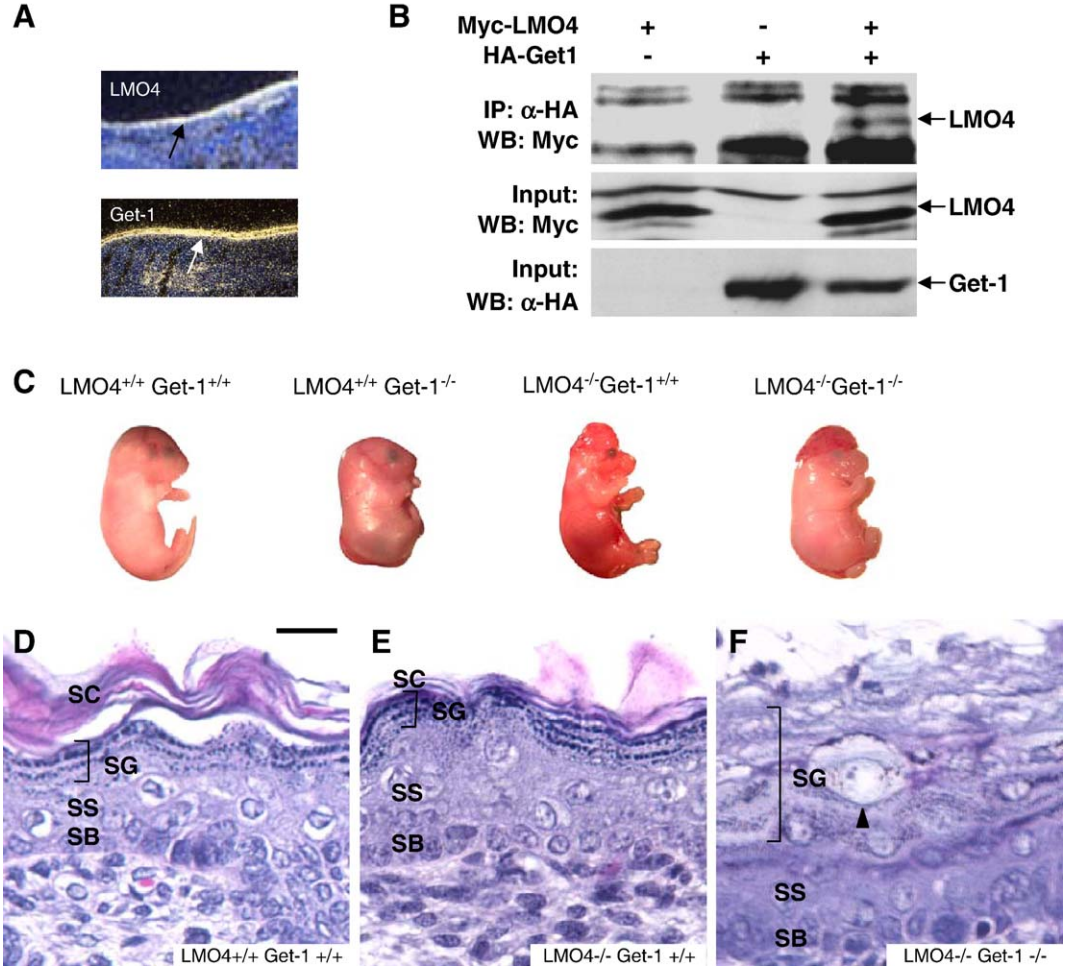

Fig. 8. Get-1 and LMO4 interact functionally to regulate terminal differentiation of the epidermis. (A) *In situ* hybridization showing expression of LMO4 and Get-1 in the developing epidermis at e15. (B) Co-immunoprecipitation of LMO4 and Get-1. Expression vectors encoding Myc tagged (MT) LMO4 and HA-tagged Get-1 were transfected into HEK293T cells either alone or together as indicated on top. The top panel shows a Western blot with MT antibody after immunoprecipitation with an HA antibody. The middle and lower panels show the input detected with MT and HA antibodies, respectively. Prominent bands in the top panel are IgG. The location of LMO4 and Get-1 is indicated with arrows. (C) Phenotypes of WT, *Get-1*$^{-/-}$, *LMO4*$^{-/-}$ and *LMO4*$^{-/-}$*Get-1*$^{-/-}$ e18.5 embryos. (D–F) Histological analysis of e18.5 backskin from WT (D), *LMO4*$^{-/-}$ (E) and *LMO4*$^{-/-}$*Get-1*$^{-/-}$ (F) mice. Scale bar: 25 μm. SB, basal layer; SC, cornified layer; SG, granular layer; SS, spinous layer.

to the adhesion (Figs. 4G–H) and barrier (Fig. 3A) defects of *Get-1*$^{-/-}$ mice.

Extracellular lipids such as free fatty acids, ceramide, cholesterol and cholesterol esters form a lamellar lipid layer between corneocytes and are essential for the barrier function of the epidermis. Several enzymes, including phospholipase A2, acid sphingomyelinase and beta-glucocerebrosidase are involved in the modification of these lipids (Elias, 2005). Among all significantly downregulated genes, we found that the most overrepresented gene ontology biological process category is lipid metabolism ($P=0.000014$), including enzymes and transporters for lipid metabolism (Fig. 6B); nearly all these genes were markedly downregulated. These include several A2 phospholipases that are critical for conversion of PL to FA (Fluhr et al., 2001), which is defective in the *Get-1*$^{-/-}$ mice (Fig. 3C). In addition, several of the downregulated enzymes, including Aloxe3, Alox12b (Jobard et al., 2002) and DGAT2 (Stone et al., 2004), have been shown in gene knockouts to be required for normal barrier function. Taken together, our results suggest that the cause of the defective barrier of *Get-1*$^{-/-}$ mice is multifactorial, involving structural components, cell–cell adhesion and lipid metabolism.

To discover potential Get-1 binding sites in differentially expressed genes, we extracted 2 kb sequences upstream of the

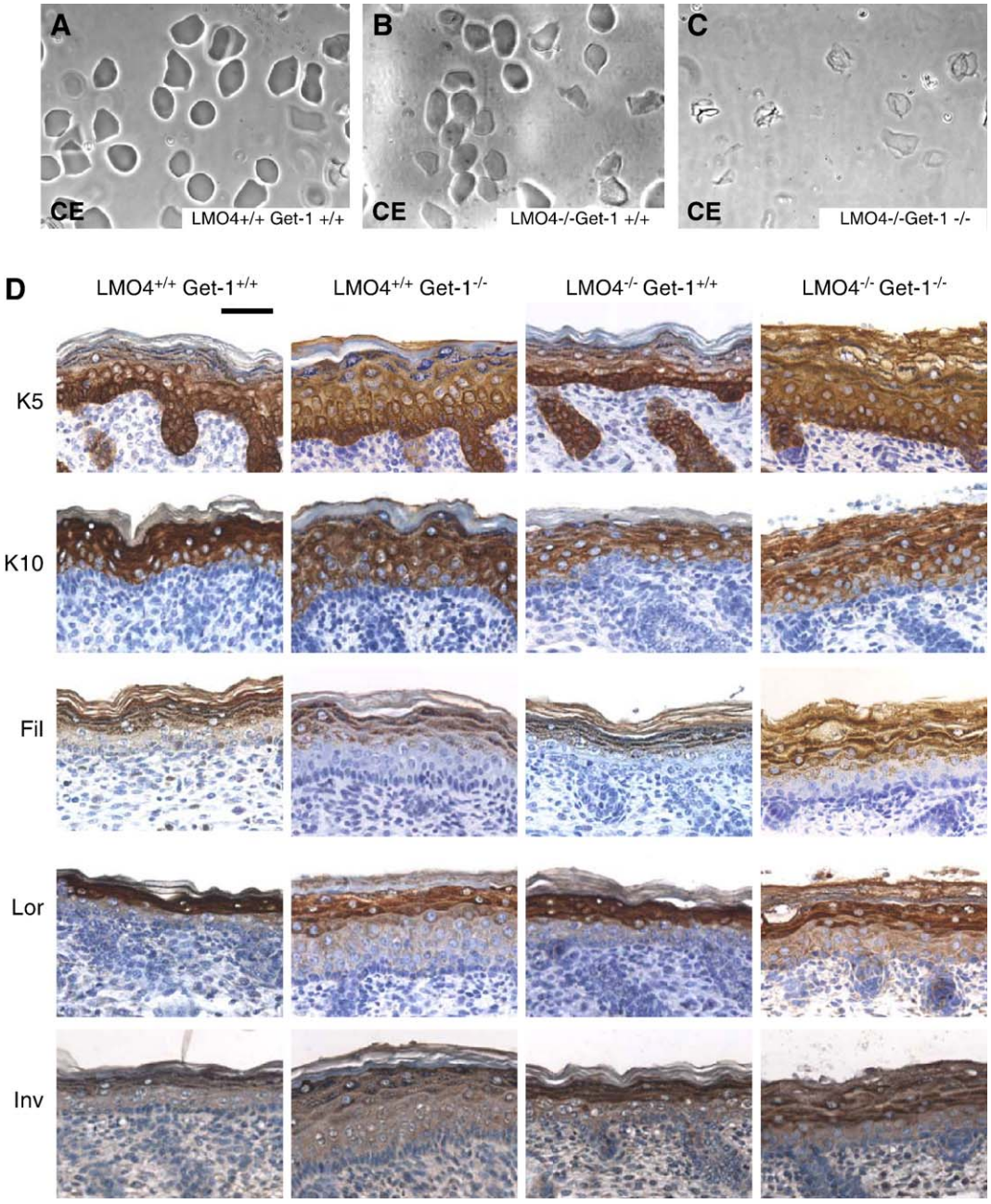

Fig. 9. Impaired stratum corneum formation in *LMO4*$^{-/-}$*Get-1*$^{-/-}$ epidermis. (A–C) Cornified envelopes isolated from e18.5 epidermis from WT (A), *LMO4*$^{-/-}$ (B) and *LMO4*$^{-/-}$*Get-1*$^{-/-}$ epidermis (C). (D) Immunostaining analysis of e18.5 epidermis from embryos of the indicated genotypes. The antibodies used are shown on the left hand. Scale bar: 50 μm. CE, cornified envelope.

transcription start site of these genes and performed positional weight matrix (PWM) analysis (Fig. 7A). Because *Tgm1* is the only known putative target gene of Get-1, we used the PWM score of the potential Get-1 binding site in the upstream region of Tgm1 (6.73) as the cut-off. Using the ConSite program (Sandelin et al., 2004), we determined the mouse–human conservation of the potential binding site as well as the surrounding genomic region. We thus found seven down-regulated genes and three upregulated genes with highly conserved sites, most of them linked to terminal differentiation of keratinocytes (Eckert et al., 2004; Higashi et al., 2004; Koch et al., 2000; Marenholz et al., 2001; Xie et al., 1993). No conserved sites were found in the non-regulated genes, indicating that the presence of high affinity Get-1 binding sites in these genes cannot be explained by chance alone (Fig. 7A). The conserved sites are all found within highly conserved genomic regions suggesting that they are part of gene-regulatory modules (Fig. 7B). Whereas this analysis suggests that some of the differentially expressed genes in the *Get-1*$^{-/-}$ epidermis could be direct target genes, further experiments with *in vivo* Get-1 binding and mutagenesis in transgenic mice are required for identification of direct target genes. We tested a random selection of potential Get-1 binding sites, some of which are in the conserved regions, and found a good correlation between binding affinity of the sites and their PWM score, thus validating previously described consensus sequence (Ting et al., 2005) (Fig. 7C). Interestingly, both up- and down-regulated genes contain conserved high-affinity binding sites, suggesting that Get-1 can act as an activator and repressor on distinct target genes (Kudryavtseva et al., 2003).

Get-1 interacts functionally with LMO4 to regulate terminal differentiation of the epidermis

We reported that Get-1 and LMO4 interact *in vitro* and have overlapping expression patterns during epidermal development (Fig. 8A) (Kudryavtseva et al., 2003). Consistent with previous results of GST pulldown assays and yeast two-hybrid interactions assays, Get-1 and LMO4 co-immunoprecipitate when transfected into HEK293T cells (Fig. 8B). However, the epidermal phenotype of *LMO4*$^{-/-}$ mice has not been characterized, and it is not known whether there are genetic interactions between *LMO4* and *Get-1* during development, including epidermal differentiation. Similar to *Get-1*$^{-/-}$ mice, *LMO4*$^{-/-}$ mice die at birth and exhibit abnormal neural tube closure, although more frequently at the anterior end (Lee et al., 2005) (Fig. 8C). In contrast to *Get-1*$^{-/-}$ mice, the epidermal barrier forms normally in *LMO4*$^{-/-}$ mice (Supplementary Fig. 2). To test the hypothesis that there are genetic interactions between *Get-1* and *LMO4*, we crossbred *LMO4*$^{+/-}$ and *Get-1*$^{+/-}$ mice to generate double knockout mice. *Get1/LMO4* double knockout mice show significantly more frequent exencephaly (100%) than that found in single knockouts (14% for *Get-1*$^{-/-}$ and 55% for *LMO4*$^{-/-}$). Similarly, open-eye phenotype was more penetrant in double knockout mice (*Get-1*$^{-/-}$, 7%; *LMO4*$^{-/-}$, 16%; and *Get-1*$^{-/-}$*LMO4*$^{-/-}$, 54%), consistent with a genetic interaction between these two genes (Fig. 8C and Supplementary Table 3). To study epidermal differentiation, we isolated backskin from e18.5 mice representing the four genotypes: WT, *Get1*$^{-/-}$, *LMO4*$^{-/-}$ and *Get1*$^{-/-}$*LMO4*$^{-/-}$. Whereas LMO4 knockout skin did not exhibit clear morphological abnormalities, compared to *Get-1*$^{-/-}$ mice, skin from double knockout mice showed marked impairment of stratum corneum formation with most cells in the top of the epidermis containing nuclei (Figs. 8D–F). Many cells showed enlarged vacuolar-like structure not normally found in the granular layer of the epidermis. This abnormality was primarily found at the anterior part of the embryo in the skin covering the head and upper body regions.

To further demonstrate the failure of epidermal terminal differentiation, we isolated cornified envelopes from WT, *LMO4*$^{-/-}$ and *Get1*$^{-/-}$*LMO4*$^{-/-}$ mice and found that although *LMO4*$^{-/-}$ cornified envelopes are normal, they were essentially absent in the double knockout mice (Figs. 9A–C). These findings indicate a severe abnormality in cornified layer formation, consistent with the expression of epidermal protein markers K5, K10, filaggrin, loricrin and involucrin, which are not normally detected in the cornified layer (Fig. 9D). The enhancement of the terminal differentiation defect in the double knockouts indicates that *Get-1* and *LMO4* interact functionally to regulate this process.

Discussion

Expression of the *Get-1* gene is initiated in the somatic ectoderm prior to formation of epidermis and continues in the proliferating cells of the developing epidermis (Fig. 8A). By birth, however, the expression level has decreased and transcripts are limited to the suprabasal compartment of the epidermis (Kudryavtseva et al., 2003). In light of the early expression of Get-1, it is interesting that the gene is critical for the terminal differentiation of keratinocytes later in embryogenesis. These results suggest that the terminal differentiation program of epidermis is initiated relatively early during skin development. In addition to epidermis, the *Get-1* gene is expressed in endoderm-derived epithelia such as that of the gut, the respiratory track and the genitourinary system (Kudryavtseva et al., 2003). Consistent with these data, we now show that the function of *Get-1* is not limited to ectodermal epithelia. The forestomach epithelium, which is highly similar to the epidermis, exhibits impaired terminal differentiation with a striking decrease in the expression of the terminal differentiation markers loricrin and filaggrin (Figs. 2S–V).

Increased epidermal thickness with expansion of all epidermal layers, especially the granular layer, is a prominent feature of the *Get-1*$^{-/-}$ phenotype. Increased proliferation of basal cell layer keratinocytes (Figs. 2P and Q) accounts for part of the epidermal thickening, but impaired cell death in the top of the granular layer may also contribute to this abnormality. Thus, we noticed frequent persistence of nuclei in the stratum corneum (Fig. 2C) and decreased caspase 14 expression in the granular layer of *Get-1*$^{-/-}$ mice (data not shown). The increased epidermal proliferation is not likely a cell-autonomous effect of Get-1 because proliferation is upregulated in the basal cell layer

at a stage when Get-1 expression is limited to the suprabasal compartment.

In addition to hyperplasia, the main epidermal abnormalities in *Get-1*$^{-/-}$ mice are found in the cornified and granular layers. Keratinocytes in the granular layer show defective flattening (Figs. 2B–C) and abnormal cell–cell adhesion (Figs. 4E–H). The cornified layer shows striking abnormalities with increased thickness, tighter cell–cell adhesion and frequent persistence of nuclei (Figs. 2C and 3B). The persistence of nuclei in the stratum corneum indicates impairment of enucleation at the top of the granular layer, an important component of the terminal differentiation program. From a functional standpoint these morphological abnormalities are significant because the barrier function of *Get-1*$^{-/-}$ mice is severely impaired (Fig. 3A).

We performed gene expression profiling to gain insights into the molecular mechanisms underlying the morphological and functional defects in the *Get-1*$^{-/-}$ epidermis (Fig. 6). The results suggest that alterations in the expression of multiple genes encoding key functional components of the terminal differentiation program contribute to defective epidermal barrier. In particular, our findings indicate that lipid abnormalities may cause defective barrier function of *Get-1*$^{-/-}$ mice. We found increased PL and decreased FA (Fig. 3C), which is implicated in maintaining normal barrier function (Elias, 2005). This finding is consistent with decreased expression of several A2 phospholipases (Fluhr et al., 2001) (Fig. 6B) that are critical for conversion of PL to FA (Fluhr et al., 2001). Altered appearance of lamellar bodies (Figs. 4I–L), as well as defective lipid lamellar formation in the cornified layer (Figs. 4C–D), also support an important role for Get-1 in regulation of epidermal lipids.

In addition to regulating lipids we found that Get-1 plays an important role in regulating transcripts involved in cell–cell adhesion, a key feature of an effective epidermal barrier. In the granular layer, there are three different cell junctions–desmosomes, tight junctions and adherence junctions–responsible for "sealing" the membranes of adjacent cells and maintaining barrier function. Knockouts of tight junction proteins (Furuse et al., 2002) and desmosomal proteins (Chidgey et al., 2001) lead to barrier defects. Therefore, the decrease in the expression of a large number of tight junction molecules, including several claudins and occludin (Figs. 6B–C), may contribute to the adhesion (Figs. 4G–H) and barrier (Fig. 3A) defects of *Get-1*$^{-/-}$ mice. Most strikingly, we found that the distribution of occludin is altered with decreased expression in the granular layer and aberrant expression in the cornified layer of *Get-1*$^{-/-}$ mice (Figs. 5D–F). Desmosomal defects could also be involved because a similar cell–cell adhesion abnormality was found in the granular layer of mice ectopically expressing Desmoglein 3 in the suprabasal compartment (Merritt et al., 2002). Consistent with this notion, Plakophilin 3 and Periplakin (Figs. 6B–C) were significantly downregulated in *Get-1*$^{-/-}$ epidermis.

Get-1 is also critical for normal expression of many structural components of the cornified envelope such as involucrin, Sprr1a, Sprrl10 and S100a3. Yet, the strength of the cornified envelope of *Get-1*$^{-/-}$ mice appeared normal (Fig. 3B). One possible explanation for this apparent dichotomy is that several structural components, including Sprr2d, Sprr2h and Repetin, were upregulated, thus compensating for the decreased expression of other components as has been suggested in loricrin knockout mice (Koch et al., 2000).

Taken together, our results strongly suggest that Get-1 plays a broad role in terminal differentiation of the epidermis and that the defective epidermal barrier of *Get-1*$^{-/-}$ mice is due to alterations in the expression of multiple genes. Consistent with this idea, the epidermal phenotype of *Get-1*$^{-/-}$ mice is striking whereas the magnitude of change for most genes in *Get-1*$^{-/-}$ epidermis is quite modest. The abnormal permeability barrier of *Get-1*$^{-/-}$ mice was previously proposed to result from decreased Tgm1 expression without the involvement of other factors involved in barrier formation (Ting et al., 2005). Our findings directly contradict these conclusions, and for several reasons we think that downregulation of Tgm1 is unlikely to fully explain the epidermal phenotype of *Get-1*$^{-/-}$ mice. First, although the barrier defect is striking, the downregulation of Tgm1 is modest, approximately two-fold. Second, although *Tgm1*$^{-/-}$ mice exhibit dramatic defects in CE formation and strength (Kuramoto et al., 2002), the fragility of the CE is decreased if anything in *Get-1*$^{-/-}$ mice (Fig. 3B), perhaps due to functional overcompensation of cornified envelope proteins such as Repetin, and certain S100 and Sprr proteins. Third, we have demonstrated altered expression of transcripts for many other key molecules involved in terminal differentiation of the epidermis and barrier formation.

To begin understanding the transcriptional mechanisms underlying gene expression changes in *Get-1*$^{-/-}$ epidermis, we have studied the frequency of Get-1 binding sites in the regulatory regions of differentially expressed genes (Fig. 7A). Although the data does not allow us to determine which of these genes are direct targets of Get-1, we have obtained clear statistical evidence that Get-1 binding sites are enriched in Get-1-responsive genes. Interestingly, however, Get-1-binding sites are absent in the conserved regions of the 2-kb of 5′ flanking sequence for most genes altered in *Get-1*$^{-/-}$ epidermis. These genes may well contain Get-1 binding sites at a greater distance from the start site. For example, a locus control region at a distance may regulate the EDC locus (Martin et al., 2004), which contains many Get-1-responsive genes (Fig. 6D). Heretofore, Klf4 is the only transcription factor conclusively shown to regulate multiple genes of the EDC (Patel et al., 2003; Segre et al., 1999). However, Get-1 appears to act differently than Klf4 because in the *Get-1*$^{-/-}$ mice some of the EDC genes are upregulated while others are downregulated. Some transcripts may also be altered in response to the barrier defect, injury and epidermal hyperplasia of *Get-1*$^{-/-}$ mice. These include Sprr2 family members, also upregulated in the loricrin knockout mice (Koch et al., 2000), as well as S100A8 and S100A9, which are downstream of AP1 (Figs. 6B and C) (Zenz et al., 2005). Interestingly, both S100A9 and Repetin transcript levels were increased at least as early as e16.5 (Supplementary Fig. 3). Based on the expression analysis, it is unlikely that alteration in the expression of other transcription factors mediate all actions of Get-1. Expression of Klf4 is not significantly decreased in the

Get-1$^{-/-}$ skin, and the modest decrease in the expression of Skn-1, a POU domain factor involved in epidermal differentiation, is unlikely to be a major contributor because singular deletion of the *Skn-1* gene causes a very mild abnormality in the terminal differentiation of the epidermis (Andersen et al., 1997).

Because we cloned Get-1 as an LMO4-interacting protein (Kudryavtseva et al., 2003), it was of interest to determine whether there are interactions between the two genes in epidermal development. Gene knockouts for both *LMO4* (Hahm et al., 2004; Lee et al., 2005; Tse et al., 2004) and *Get-1* (Ting et al., 2003a) result in neural tube defects, which support the possibility that interaction between the two proteins is important. Interestingly, however, the epidermis of *LMO4*$^{-/-}$ mice appears normal (Figs. 8D–E; Supplementary Fig. 2), indicating that under non-perturbed conditions, Get-1 can function without LMO4. Yet, deletion of the *Get-1* gene in the absence of the *LMO4* gene leads to a much more striking phenotype with a dramatic impairment in the formation of the cornified layer, and a markedly abnormal granular layer (Figs. 8F and 9). Furthermore, the penetrance of the eye-open and exencephaly phenotypes is significantly increased in the double knockouts compared to either single knockout (Supplementary Table 3). Together, these findings demonstrate genetic interactions between *LMO4* and *Get-1* and based on the ability of these proteins to interact *in vitro*, it is tempting to speculate that the functional interaction results from altered transcriptional complexes in which both LMO4 and Get-1 participate. It is also possible that LMO4 and Get-1 play sequential roles at different stages in the control of epidermal development.

In conclusion, our results suggest that *Get-1* plays an important role in the terminal differentiation and barrier function of the epidermis by regulating multiple genes, including those of the EDC complex encoding structural proteins, enzymes controlling extracellular lipid metabolism, cell adhesion molecules and protein-modifying enzymes. Furthermore, *Get-1* interacts functionally with *LMO4* to regulate terminal differentiation of the epidermis. The broad range of genes whose expression is altered by *Get-1* deletion implicates Get-1 proximally in a complex pathway that ultimately coordinates different aspects of the terminal differentiation program in epidermis.

Acknowledgments

We thank Xing Dai and Liz Rugg for reading the manuscript, Ozgene for knockout mice and Kaye Starr Lam for technical help. This work was supported by NIH Grant AR44882 (BA), the California Breast Cancer Research Program (ZY and XX) and the Breast Cancer Research Program of the United States Army Medical Research and Material Command (ZL).

Appendix A. Supplementary data

Supplementary data associated with this article can be found in the online version at doi:10.1016/j.ydbio.2006.07.015.

References

Andersen, B., Pearse II, R.V., Jenne, K., Sornson, M., Lin, S.C., Bartke, A., Rosenfeld, M.G., 1995. The Ames dwarf gene is required for Pit-1 gene activation. Dev. Biol. 172, 495–503.

Andersen, B., Weinberg, W.C., Rennekampff, O., McEvilly, R.J., Bermingham Jr., J.R., Hooshmand, F., Vasilyev, V., Hansbrough, J.F., Pittelkow, M.R., Yuspa, S.H., Rosenfeld, M.G., 1997. Functions of the POU domain genes Skn-1a/i and Tst-1/Oct-6/SCIP in epidermal differentiation. Genes Dev. 11, 1873–1884.

Baldi, P., Long, A.D., 2001. A Bayesian framework for the analysis of microarray expression data: regularized t-test and statistical inferences of gene changes. Bioinformatics 17, 509–519.

Bray, S.J., Kafatos, F.C., 1991. Developmental function of Elf-1: an essential transcription factor during embryogenesis in *Drosophila*. Genes Dev. 5, 1672–1683.

Candi, E., Schmidt, R., Melino, G., 2005. The cornified envelope: a model of cell death in the skin. Nat. Rev., Mol. Cell Biol. 6, 328–340.

Chidgey, M., Brakebusch, C., Gustafsson, E., Cruchley, A., Hail, C., Kirk, S., Merritt, A., North, A., Tselepis, C., Hewitt, J., Byrne, C., Fassler, R., Garrod, D., 2001. Mice lacking desmocollin 1 show epidermal fragility accompanied by barrier defects and abnormal differentiation. J. Cell Biol. 155, 821–832.

Dennis Jr., G., Sherman, B.T., Hosack, D.A., Yang, J., Gao, W., Lane, H.C., Lempicki, R.A., 2003. DAVID: database for annotation, visualization, and integrated discovery. Genome Biol. 4, P3.

Eckert, R.L., Broome, A.M., Ruse, M., Robinson, N., Ryan, D., Lee, K., 2004. S100 proteins in the epidermis. J. Invest. Dermatol. 123, 23–33.

Elias, P.M., 2005. Stratum corneum defensive functions: an integrated view. J. Invest. Dermatol. 125, 183–200.

Fluhr, J.W., Kao, J., Jain, M., Ahn, S.K., Feingold, K.R., Elias, P.M., 2001. Generation of free fatty acids from phospholipids regulates stratum corneum acidification and integrity. J. Invest. Dermatol. 117, 44–51.

Furuse, M., Hata, M., Furuse, K., Yoshida, Y., Haratake, A., Sugitani, Y., Noda, T., Kubo, A., Tsukita, S., 2002. Claudin-based tight junctions are crucial for the mammalian epidermal barrier: a lesson from claudin-1-deficient mice. J. Cell Biol. 156, 1099–1111.

Hahm, K., Sum, E.Y., Fujiwara, Y., Lindeman, G.J., Visvader, J.E., Orkin, S.H., 2004. Defective neural tube closure and anteroposterior patterning in mice lacking the LIM protein LMO4 or its interacting partner Deaf-1. Mol. Cell. Biol. 24, 2074–2082.

Hardman, M.J., Sisi, P., Banbury, D.N., Byrne, C., 1998. Patterned acquisition of skin barrier function during development. Development 125, 1541–1552.

Higashi, Y., Fuda, H., Yanai, H., Lee, Y., Fukushige, T., Kanzaki, T., Strott, C. A., 2004. Expression of cholesterol sulfotransferase (SULT2B1b) in human skin and primary cultures of human epidermal keratinocytes. J. Invest. Dermatol. 122, 1207–1213.

Jobard, F., Lefevre, C., Karaduman, A., Blanchet-Bardon, C., Emre, S., Weissenbach, J., Ozguc, M., Lathrop, M., Prud'homme, J.F., Fischer, J., 2002. Lipoxygenase-3 (ALOXE3) and 12(R)-lipoxygenase (ALOX12B) are mutated in non-bullous congenital ichthyosiform erythroderma (NCIE) linked to chromosome 17p13.1. Hum. Mol. Genet. 11, 107–113.

Koch, P.J., de Viragh, P.A., Scharer, E., Bundman, D., Longley, M.A., Bickenbach, J., Kawachi, Y., Suga, Y., Zhou, Z., Huber, M., Hohl, D., Kartasova, T., Jarnik, M., Steven, A.C., Roop, D.R., 2000. Lessons from loricrin-deficient mice: compensatory mechanisms maintaining skin barrier function in the absence of a major cornified envelope protein. J. Cell Biol. 151, 389–400.

Kudryavtseva, E.I., Sugihara, T.M., Wang, N., Lasso, R.J., Gudnason, J.F., Lipkin, S.M., Andersen, B., 2003. Identification and characterization of Grainyhead-like epithelial transactivator (GET-1), a novel mammalian Grainyhead-like factor. Dev. Dyn. 226, 604–617.

Kuramoto, N., Takizawa, T., Matsuki, M., Morioka, H., Robinson, J.M., Yamanishi, K., 2002. Development of ichthyosiform skin compensates for defective permeability barrier function in mice lacking transglutaminase 1. J. Clin. Invest. 109, 243–250.

Law, S., Wertz, P.W., Swartzendruber, D.C., Squier, C.A., 1995. Regional variation in content, composition and organization of porcine epithelial

barrier lipids revealed by thin-layer chromatography and transmission electron microscopy. Arch. Oral Biol. 40, 1085–1091.

Lee, S.K., Jurata, L.W., Nowak, R., Lettieri, K., Kenny, D.A., Pfaff, S.L., Gill, G.N., 2005. The LIM domain-only protein LMO4 is required for neural tube closure. Mol. Cell. Neurosci. 28, 205–214.

Lin, K.K., Chudova, D., Hatfield, G.W., Smyth, P., Andersen, B., 2004. Identification of hair cycle-associated genes from time-course gene expression profile data by using replicate variance. Proc. Natl. Acad. Sci. U. S. A. 101, 15955–15960.

Long, A.D., Mangalam, H.J., Chan, B.Y., Tolleri, L., Hatfield, G.W., Baldi, P., 2001. Improved statistical inference from DNA microarray data using analysis of variance and a Bayesian statistical framework. Analysis of global gene expression in Escherichia coli K12. J. Biol. Chem. 276, 19937–19944.

Lu, Z., Lam, K.S., Wang, N., Xu, X., Cortes, M., Andersen, B., 2006. LMO4 can interact with Smad proteins and modulate transforming growth factor-beta signaling in epithelial cells. Oncogene 25, 2920–2930.

Mace, K.A., Pearson, J.C., McGinnis, W., 2005. An epidermal barrier wound repair pathway in *Drosophila* is mediated by grainy head. Science 308, 381–385.

Marenholz, I., Zirra, M., Fischer, D.F., Backendorf, C., Ziegler, A., Mischke, D., 2001. Identification of human epidermal differentiation complex (EDC)-encoded genes by subtractive hybridization of entire YACs to a gridded keratinocyte cDNA library. Genome Res. 11, 341–355.

Martin, N., Patel, S., Segre, J.A., 2004. Long-range comparison of human and mouse Sprr loci to identify conserved noncoding sequences involved in coordinate regulation. Genome Res. 14, 2430–2438.

Merritt, A.J., Berika, M.Y., Zhai, W., Kirk, S.E., Ji, B., Hardman, M.J., Garrod, D.R., 2002. Suprabasal desmoglein 3 expression in the epidermis of transgenic mice results in hyperproliferation and abnormal differentiation. Mol. Cell. Biol. 22, 5846–5858.

Nickoloff, B.J., 2006. Keratinocytes regain momentum as instigators of cutaneous inflammation. Trends Mol. Med. 12, 102–106.

Patel, S., Kartasova, T., Segre, J.A., 2003. Mouse Sprr locus: a tandem array of coordinately regulated genes. Mamm. Genome 14, 140–148.

Sandelin, A., Wasserman, W.W., Lenhard, B., 2004. ConSite: Web-based prediction of regulatory elements using cross-species comparison. Nucleic Acids Res. 32, W249–W252.

Schwenk, F., Baron, U., Rajewsky, K., 1995. A cre-transgenic mouse strain for the ubiquitous deletion of loxP-flanked gene segments including deletion in germ cells. Nucleic Acids Res. 23, 5080–5081.

Segre, J., 2003. Complex redundancy to build a simple epidermal permeability barrier. Curr. Opin. Cell Biol. 15, 776–782.

Segre, J.A., Bauer, C., Fuchs, E., 1999. Klf4 is a transcription factor required for establishing the barrier function of the skin. Nat. Genet. 22, 356–360.

Shwayder, T., Akland, T., 2005. Neonatal skin barrier: structure, function, and disorders. Dermatol. Ther. 18, 87–103.

Stone, S.J., Myers, H.M., Watkins, S.M., Brown, B.E., Feingold, K.R., Elias, P.M., Farese Jr., R.V., 2004. Lipopenia and skin barrier abnormalities in DGAT2-deficient mice. J. Biol. Chem. 279, 11767–11776.

Sugihara, T.M., Bach, I., Kioussi, C., Rosenfeld, M.G., Andersen, B., 1998. Mouse deformed epidermal autoregulatory factor 1 recruits a LIM domain factor, LMO-4, and CLIM coregulators. Proc. Natl. Acad. Sci. U. S. A. 95, 15418–15423.

Ting, S.B., Wilanowski, T., Auden, A., Hall, M., Voss, A.K., Thomas, T., Parekh, V., Cunningham, J.M., Jane, S.M., 2003a. Inositol- and folate-resistant neural tube defects in mice lacking the epithelial-specific factor Grhl-3. Nat. Med. 9, 1513–1519.

Ting, S.B., Wilanowski, T., Cerruti, L., Zhao, L.L., Cunningham, J.M., Jane, S.M., 2003b. The identification and characterization of human sister-of-mammalian Grainyhead (SOM) expands the Grainyhead-like family of developmental transcription factors. Biochem. J. 370, 953–962.

Ting, S.B., Caddy, J., Hislop, N., Wilanowski, T., Auden, A., Zhao, L.L., Ellis, S., Kaur, P., Uchida, Y., Holleran, W.M., Elias, P.M., Cunningham, J.M., Jane, S.M., 2005. A homolog of *Drosophila* grainy head is essential for epidermal integrity in mice. Science 308, 411–413.

Tse, E., Smith, A.J., Hunt, S., Lavenir, I., Forster, A., Warren, A.J., Grutz, G., Foroni, L., Carlton, M.B., Colledge, W.H., Boehm, T., Rabbitts, T.H., 2004. Null mutation of the Lmo4 gene or a combined null mutation of the Lmo1/Lmo3 genes causes perinatal lethality, and Lmo4 controls neural tube development in mice. Mol. Cell. Biol. 24, 2063–2073.

Vega, V.B., Bangarusamy, D.K., Miller, L.D., Liu, E.T., Lin, C.Y., 2004. BEARR: batch extraction and analysis of *cis*-regulatory regions. Nucleic Acids Res. 32, W257–W260.

Xie, M., Sesko, A.M., Low, M.G., 1993. Glycosylphosphatidylinositol-specific phospholipase D is localized in keratinocytes. Am. J. Physiol. 265, C1156–C1168.

Zenz, R., Eferl, R., Kenner, L., Florin, L., Hummerich, L., Mehic, D., Scheuch, H., Angel, P., Tschachler, E., Wagner, E.F., 2005. Psoriasis-like skin disease and arthritis caused by inducible epidermal deletion of Jun proteins. Nature 437, 369–375.